Magnetic-superconducting phase diagram of $Eu_{2-x}Ce_xRuSr_2Cu_2O_{10-\delta}$

I. Felner, U. Asaf, and E. Galstyan
Racah Institute of Physics, The Hebrew University, Jerusalem, 91904, Israel
(Received 26 November 2001; revised manuscript received 21 March 2002; published 24 June 2002)

$Eu_{2-x}Ce_xRuSr_2Cu_2O_{10-\delta}$ (Ru-2122) is the first Cu-O-based system in which superconductivity (SC) in the CuO_2 planes and *weak* ferromagnetism (WFM) in the Ru sublattice coexist. The hole doping in the CuO_2 planes is controlled by appropriate variation of the Ce concentration. SC occurs for Ce contents of 0.4–0.8, with the highest $T_C=35$ K for Ce=0.6. The as-prepared non-SC $EuCeRuSr_2Cu_2O_{10}$ ($x=1$) sample exhibits magnetic irreversibility below $T_{irr}=125$ K and orders *antiferromagnetically* (AFM) at $T_M=165$ K. The saturation moment at 5 K is $M_{sat}=0.89\mu_B$/Ru close to the expected $1\mu_B$ for the low-spin state of Ru^{5+}. Annealing under oxygen pressures does not affect these parameters, whereas depletion of oxygen shifts both T_{irr} and T_M up to 169 and 215 K, respectively. Systematic magnetic studies of $Eu_{2-x}Ce_xRuSr_2Cu_2O_{10-\delta}$ show that T_M, T_{irr}, and M_{sat} decrease with x, and the full Ce-dependent magnetic-SC phase diagram is presented. A simple model for the SC state is proposed. We interpret the magnetic behavior in the framework of our ac and dc magnetic studies, and argue that (i) the system becomes AFM ordered at T_M; (b) at $T_{irr}<T_M$, WFM is induced by the canting of the Ru moments: and (c) at lower temperatures, the appropriate samples become SC at T_C. The magnetic features are not affected by the SC state, and the two states coexist.

DOI: 10.1103/PhysRevB.66.024503 PACS number(s): 74.25.Ha, 75.70.Cn

I. INTRODUCTION

Much attention has been focused on a phase resembling the superconducting $RBa_2Cu_3O_7$ (R=rare earth) materials, having the composition $R_{2-x}Ce_xMSr_2Cu_2O_{10}$ (M-2122, M=Nb, Ru, or Ta).[1] The tetragonal M-2122 structure (space group $I4/mmm$) evolves from the $RBa_2Cu_3O_7$ structure by inserting a fluorite-type $R_{1.5}Ce_{0.5}O_2$ layer instead of the R layer in $RBa_2Cu_3O_7$, thus shifting alternate perovskite blocks by $(a+b)/2$. The M ions reside in the Cu(1) site, and only one distinct Cu site [corresponding to Cu(2) in $RBa_2Cu_3O_7$] with fivefold pyramidal coordination exists. The hole doping of the Cu-O planes, which results in metallic behavior and superconductivity (SC), can be optimized with appropriate variation of the R/Ce ratio.[2] SC occurs for Ce contents of 0.4–0.8, and the highest T_C was obtained for Ce=0.6. The Nb-2122 and Ta-2122 materials are SC with $T_C\sim 28-30$ K.[1]

Coexistence of weak ferromagnetism (WFM) and SC was discovered few years ago in $R_{1.5}Ce_{0.5}RuSr_2Cu_2O_{10}$ (R=Eu and Gd, Ru-2122) layered cuprate systems[3–6] and, more recently,[7] in $GdSr_2RuCu_2O_8$ (Ru-1212). The SC charge carriers originate from the CuO_2 planes, and the WFM state is confined to the Ru layers. In both systems, the magnetic order does not vanish when SC sets in at T_C and remains unchanged and coexists with the SC state. The Ru-2122 materials (for R=Eu) display a magnetic transition at $T_M=125-180$ K and bulk SC below $T_C=32-50$ K ($T_M>T_C$) depending on oxygen concentration and sample preparation.[6] SC survives because the Ru moments probably align in the basal planes, which are practically decoupled from the CuO_2 planes, so that there is no pair breaking. Specific heat studies show a sizable typical jump at T_C, and the magnitude of the $\Delta C/T$ (0.08 mJ/gK^2) indicates clearly the presence of bulk SC.[8] The specific heat anomaly is independent of the applied magnetic field. Scanning tunneling spectroscopy,[3] muon-spin rotation,[9] and magneto-optic experiments[10] have demonstrated that all materials are microscopically uniform with no evidence for spatial phase separation of superconducting and magnetic regions. That is, both states coexist intrinsically on the microscopic scale.

In the Ru-2122 system, the WFM state, as well as the irreversibility phenomena, arises as a result of an antisymmetric exchange coupling of the Dzyaloshinsky-Moriya (DM) type[3] between neighboring Ru moments, induced by a local distortion that breaks the tetragonal symmetry of the RuO_6 octahedra. Due to this DM interaction, the field causes the adjacent spins to cant slightly out of their original direction and to align a component of the moments with the direction of the applied field. Below the irreversible temperature (T_{irr}), which is defined as the merging temperature of the zero-field- (ZFC) and field-cooled (FC) curves, the Ru-Ru interactions begin to dominate, leading to reorientation of the Ru moments, which leads to a peak in the magnetization curves. The Ce concentration affects the hole carrier concentration as a result the SC properties and the T_C values of the $R_{2-x}Ce_xRuSr_2Cu_2O_{10-\delta}$ system. The remaining unresolved question concerns the effect of Ce concentration on magnetic properties of this system. It was shown that the position of the peak in ZFC magnetization shifts to higher temperature with increasing Ce content,[11] however, detailed magnetic features of this system are lacking.

In attempting to understand the mechanism of SC and WFM in the Ru-2122 system, an approach involving a systematic investigation of the magnetic properties of $Eu_{2-x}Ce_xRuSr_2Cu_2O_{10-\delta}$ for $0.4<x<1$ was employed. Eu^{3+} is used in order to avoid significant paramagnetic contribution of Gd^{3+}. This paper is organized as follows: (a) We first show the effect of Ce on the SC properties and compare between the two Ru-2122 $La_{2-x}Sr_xCuO_4$ systems. (b) We present the magnetic properties of the non-SC $EuCeRuSr_2Cu_2O_{10}$ ($x=1$) material, in which the oxygen concentration is fixed. Annealing under high oxygen pressure does not alter the magnetic properties. (c) We exhibit a sys-

tematic study of the influence of Ce concentration on the magnetic parameters of $Eu_{2-x}Ce_xRuSr_2Cu_2O_{10-\delta}$ and construct the full SC-magnetic phase diagram. (d) A qualitative model of the magnetic structure in the Ru-2122 system is discussed.

II. EXPERIMENTAL DETAILS

Ceramic samples with nominal composition $Eu_{2-x}Ce_xRuSr_2Cu_2O_{10-\delta}$ ($x=0.4-1$) were prepared by a solid-state reaction technique. Prescribed amounts of Eu_2O_3, CeO_2, $SrCO_3$, Ru, and CuO were mixed and pressed into pellets and preheated at 1000 °C for about 1 day at atmospheric pressure. The products were cooled, reground and sintered at 1050 °C for 50 h in a slightly pressurized oxygen atmosphere (~1.1 atm), and then furnace cooled to ambient temperature [as-prepared asp samples]. All the asp materials reported were prepared at the same time and under the same conditions. Part of the asp $EuCeRuSr_2Cu_2O_{10}$ sample was reheated for 24 h at 800 °C under high pressure of oxygen (60 atm) and another part was quenched from 1050 °C to room temperature, denoted as hop and quenched materials, respectively. Determination of the absolute oxygen content in the asp Ru-2122 material, as well as in the hop and quenched samples, is difficult because CeO_2 is not completely reducible to a stoichiometric oxide when heated to high temperatures.

Powder x-ray diffraction (XRD) measurements confirmed the purity of the compounds (~97%) and indicate, within the instrumental accuracy, that all samples have the same lattice parameters $a=3.846(1)$ Å and $c=28.72(1)$ Å, in excellent agreement with Ref. 3. Here ZFC and FC dc magnetic measurements in the range of 5–300 K were performed in a commercial (Quantum Design) superconducting quantum interference device (SQUID) magnetometer. The resistance was measured by a standard four-contact probe, and the ac susceptibility was measured by a homemade probe with exitation frequency and amplitude of 733 Hz and 30 mOe, respectively, both inserted in the SQUID magnetometer.

III. EXPERIMENTAL RESULTS AND DISCUSSION

Due to the similarity of the ionic radii of Eu^{3+} (0.94 Å) and Ce^{4+} (0.87 Å) and within the instrumental accuracy, the lattice parameters of $Eu_{2-x}Ce_xRuSr_2Cu_2O_{10-\delta}$ are independent of Ce content. The detailed crystal structure and the atomic positions Ru-2122 were studied by synchrotron x-ray diffraction[12] and neutron diffraction[13] experiments, which show that the RuO_6 octahedra are rotated ~14° around the c axis and that this rotation is essentially the same for $x=1$ and $x=0.6$ as well as for Ru-1212. There is no evidence for supercell peaks in the Ru-2122 samples.

A. Superconductivity in the $Eu_{2-x}Ce_xRuSr_2Cu_2O_{10-\delta}$ system

The temperature dependence of the normalized ac susceptibility curves (at $H_{dc}=0$) for the $Eu_{2-x}Ce_xRuSr_2Cu_2O_{10-\delta}$ system are presented in Fig. 1. It is readily observed that the $x=1$ and 0.9 samples are not SC and that SC occurs for Ce contents of $x=0.8-0.4$. Figure 2 exhibits the onset of SC

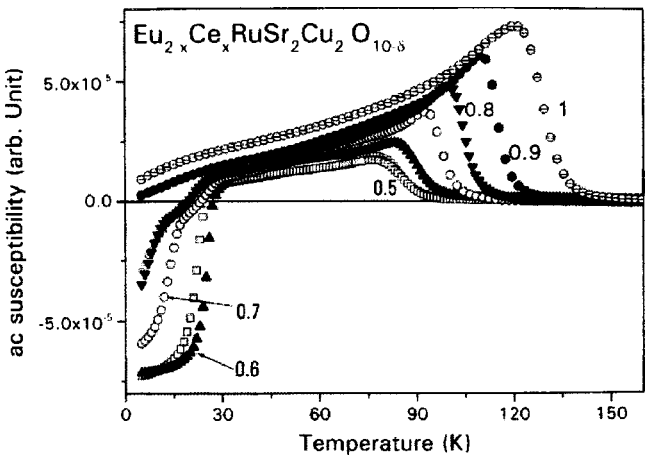

FIG. 1. Normalized ac susceptibility, measured at $H_{dc}=0$ of the asp $Eu_{2-x}Ce_xRuSr_2Cu_2O_{10-\delta}$ samples. Note that the two $x=1$ and $x=0.9$ materials are magnetically ordered only.

deduced from these ac plots which exhibit a bell-shaped behavior with a peak at 35 K for Ce=0.6. Similar values are obtained by our resistivity measurements (not shown). A similar bell-shaped behavior was observed in the $Eu_{2-x}Ce_xNbSr_2Cu_2O_{10-\delta}$ ($x=0.4-1$) system, which serves as reference materials. It is apparent in Fig. 1 that the SC transitions are much broader than those observed in many other high-temperature superconducting (HTSC) materials. This transition width is comparable to our previous resistivity data[3,6] and with Ref. 11. Such a broadening is observed also in some underdoped Cu-based high-T_C materials where inhomogeniety in the oxygen concentration causes a distribution in the T_C values. In addition, the SC transition width may be due to the spontaneous vortex state discussed in detail in Ref. 4. In the next section we suggest an intuitive explanation as to why the M-2122 (M=Ru, Ta, and Nb) materials are superconducting.

Given the variety of crystal structures and chemical methods used to introduce holes into the CuO_2 layers, it is well established that a ''generic'' electronic phase diagram can be

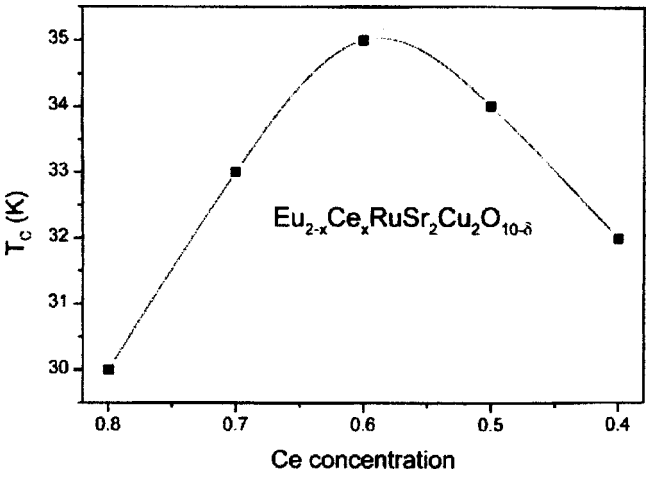

FIG. 2. Bell-shaped SC onset temperature as a function of Ce content.

sketched for all compounds. The hole (or carrier) density (p) in the CuO_2 planes or deviation of the formal Cu valence from Cu^{2+} is a primary parameter, which affects T_C in most of the HTSC compounds. In the well-established phase diagram $La_{2-x}Sr_xCuO_4$, the stoichiometric parent La_2CuO_4 is antiferromagnetic (AFM) and insulating. The magnetic interactions are well described by a simple Heisenberg model, with a large exchange interaction ($J=1500$ K) value. In $La_{2-x}Sr_xCuO_4$ the charge carrier concentration can be varied by replacing Sr^{2+} for La^{3+} (or by a change of oxygen concentration in $YBa_2Cu_3O_z$). The variation of T_C as a function of hole doping exhibits a bell-shaped behavior, with a peak for the optimally doped material ($x=0.15$ for $La_{2-x}Sr_xCuO_4$).

The Eu, Ce, and Ru ion valences in $Eu_{1.5}Ce_{0.5}RuSr_2Cu_2O_{10-\delta}$ have been studied by Mössbauer spectroscopy (MS) and X-ray-absorption spectroscopy (XAS) techniques.[14,15] MS performed at 90 and 300 K on ^{151}Eu shows a single narrow line with an isomer shift of 0.69(2) mm/s, indicating that the Eu ions are trivalent with a nonmagnetic $J=0$ ground state XAS taken at L_{III} edges of Ce shows also that Ce is tetravalent. XAS taken at the K edge of Ru, at room temperature, indicates clearly that the Ru ions are pentavalent.[14,15] It is also apparent that bulk SC in the M-2122 system appears only for pentavalent M ions and the Nb-2122 and Ta-2122 materials are SC with $T_C \sim 28-30$ K.[1]

We argue that the $RCeMSr_2Cu_2O_{10}$ ($R=$ Eu or Gd and $R/Ce=1$) samples serve as the parent stoichiometric insulator compounds (similar to La_2CuO_4). Since the valences of R^{3+}, Ce^{4+}, Ru^{5+}, Sr^{2+}, Cu^{2+}, and O^{2-} are conclusive, a straightforward valence counting yields a fixed oxygen concentration of 10. Hole doping of the Cu-O planes, which results in metallic behavior and SC, can be optimized with appropriate variation of the R^{3+}/Ce^{4+} ratio (trivalent R^{3+} ions are replaced for Ce^{4+}). SC occurs for Ce contents of 0.4–0.8, and the optimally doped sample is obtained for Ce $=0.6$. In fact, unlike the $La_{2-x}Sr_xCuO_4$ system, this substitution does not appear to significantly alter the hole concentration (p) on the Cu-O planes. This is apparent in Fig. 2, which shows that the change of x from 0.8 to 0.6 results in a small increase in T_C. Indeed, if all the carriers were induced into the Cu-O planes, then for the underdoped ($x=0.8$) to the optimally doped ($x=0.6$) samples, p should vary by 0.2 and result in a large shift in T_C, as observed in $La_{2-x}Sr_xCuO_4$ and in other HTSC materials. It is thus possible that in all $M=2122$ compounds, the extra holes introduced by reducing the Ce content are partially compensated for by depletion of oxygen[11] and in $R_{2-x}Ce_xRuSr_2Cu_2O_{10-\delta}$ the oxygen deficiency (δ) increases with R^{3+}. This partial hole doping mechanism is also supported by neutron diffraction on $Gd_{1.3}Ce_{0.7}RuSr_2Cu_2O_{10-\delta}$, from which one finds $\delta=0.22$, instead of 0.3 required by charge neutrality.[13] In the case of $M=$ Ru, $EuCeRuSr_2Cu_2O_{10}$ is magnetically ordered at $T_M=165$ K, and the next section deals with its detailed magnetic behavior.

B. Effect of oxygen on the magnetic behavior of $EuCeRuSr_2Cu_2O_{10}$

$EuCeRuSr_2Cu_2O_{10}$ is not SC and is only magnetically ordered (Fig. 1). ZFC and FC dc magnetic measurements for the parent asp sample were performed over a broad range of applied magnetic fields, and typical M/H curves measured at 50 Oe are shown in Fig. 3. The two curves merge at $T_{irr}=125$ K. Note the ferromagneticlike shape of the FC branches. T_M(Ru) is not at T_{irr}. The $M/H(T)$ curves do not lend themselves to an easy determination of T_M(Ru), and T_M(Ru) $=165$ K was obtained directly from the temperature dependence of the saturation moment (M_{sat}), discussed below. [An alternative way to determine T_M(Ru) is to cool the material from above T_M, under a small *negative* magnetic field (say -5 Oe), which aligns the Ru sublattice. At low temperatures, a small *positive* (5 Oe) is applied. Due to the high anisotropy, the Ru moments remain opposite the field direction up to T_M. The measured negative $M(T)$ curve becomes zero at T_M]. T_{irr} is field dependent and shifted to lower temperatures with the applied field. $T_{irr}=91$, 64, 39, 28, and 14 K for $H=250$, 500, 1000, 2000, and 3000 Oe, respectively. For higher external fields the irreversibility is washed out, and both ZFC and FC curves collapse to a single ferromagneticlike behavior. It appears that the magnetic properties of Ru in $EuCeRuSr_2Cu_2O_{10}$ are all *enhanced*, as compared to the asp $Eu_{2-x}Ce_xRuSr_2Cu_2O_{10-\delta}$ samples with $x<1$, and the effect of Ce concentration on the magnetic parameters of the Ru sublattice will be discussed below.

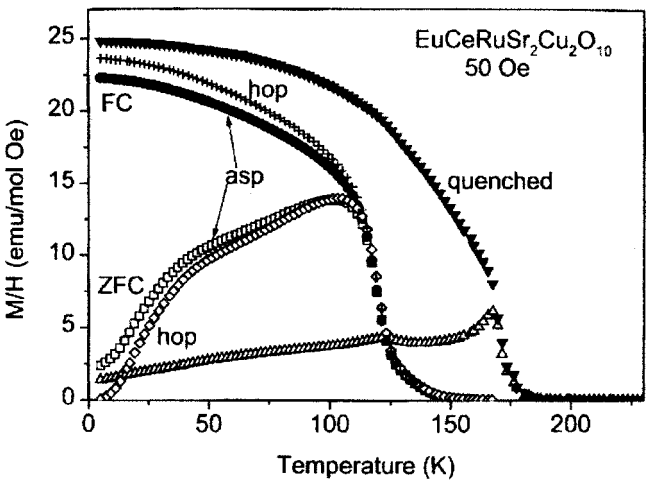

FIG. 3. ZFC and FC susceptibility curves for $EuCeRuSr_2Cu_2O_{10}$ samples, asp, annealed under 60 oxygen atmosphere and quenched materials measured at 50 Oe.

Similar $M/H(T)$ curves were measured for the oxygen annealed (hop) sample, and Fig. 3 shows that both T_{irr} and T_M(Ru) remain unchanged. This is in contrast to $Eu_{1.5}Ce_{0.5}RuSr_2Cu_2O_{10-\delta}$ where annealing under oxygen pressure affects T_{irr} and T_M(Ru) and shifts them to higher temperatures.[5,6] As stated above, the oxygen concentration in $EuCeRuSr_2Cu_2O_{10}$ is fixed and does not change during the annealing process. On the other hand, during the quenching process, a small amount of oxygen is depleted and both T_{irr} and T_M(Ru) are shifted to 169 and 215 K, respectively (Fig. 3), similar to that reported in Ref. 5. It is reminiscent of the magnetic phase diagram of $YBa_2Cu_3O_z$, where the depletion of oxygen increases the magnetic transition of the CuO_2 planes. This shift proves that the magnetic transition at 165

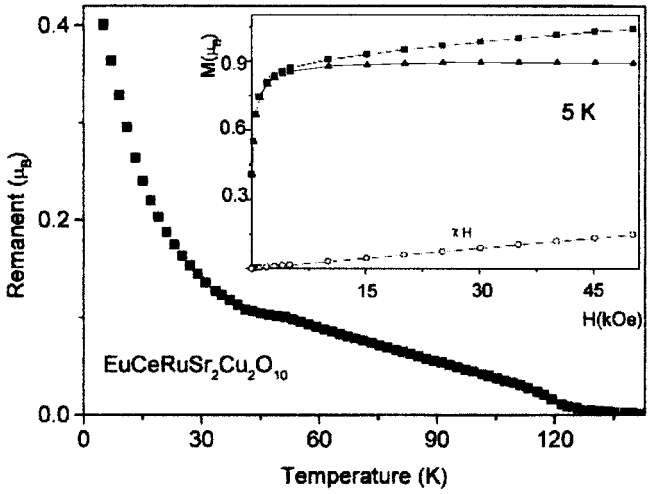

FIG. 4. Temperature dependence of the 5 K remnant moment of $EuCeRuSr_2Cu_2O_{10}$. The inset shows the high-field magnetization and the saturation moment at 5 K.

K of $EuCeRuSr_2Cu_2O_{10}$ is intrinsic and not from the $SrRuO_3$ impurity phase, which has a similar T_M(Ru).

$M(H)$ measurements at various temperatures for the asp, hop, and quenched samples have been carried out, and the results obtained for the asp sample are exhibited in Figs. 4–6. All $M(H)$ curves below T_M are strongly dependent on the field (up to 2–4 kOe), until a common slope is reached (Fig. 4, inset). $M(H)$ can be described as $M(H)=M_{\rm sat}+\chi H$, where $M_{\rm sat}$ corresponds to the WFM contribution of the Ru sublattice and χH is the linear paramagnetic contribution of Eu and Cu. The saturation moment obtained at 5 K is $M_{\rm sat}=0.89(1)\mu_B$. Similar $M(H)$ curves have been measured at various temperatures, and Fig. 5 (inset) shows the decrease of $M_{\rm sat}$ with temperature. $M_{\rm sat}$ becomes zero at T_M(Ru)$=165(2)$. Similar $M_{\rm sat}$ and T_M(Ru) values were obtained for the hop material. However, for the quenched material, the saturation moment at 5 K remains unchanged, but T_M is shifted to 215(2) K. Thus only the magnetic transitions

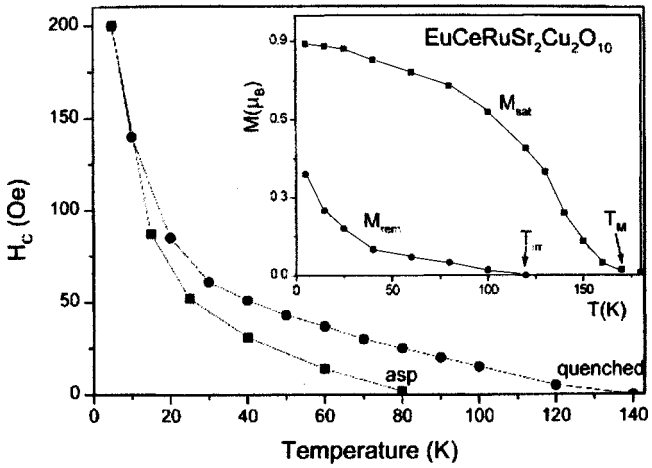

FIG. 5. Coercive field H_C as function of temperature for asp and quenched $EuCeRuSr_2Cu_2O_{10}$ samples. The inset shows the temperature dependence of the saturation and the remnant moments.

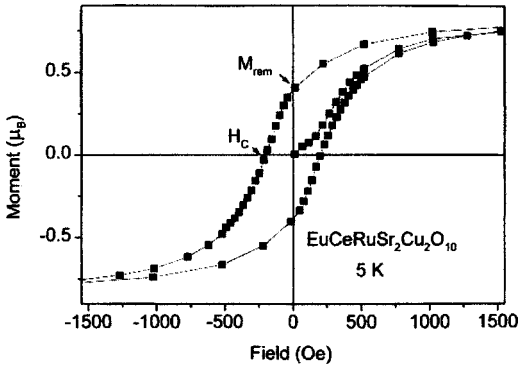

FIG. 6. Hysteresis low-field loop at 5 K.

are sensitive to the oxygen concentration. The measured $M_{\rm sat}=0.89\mu_B$ is somewhat smaller than the fully saturated moment $1\mu_B$ expected for the low-spin state of Ru^{5+}—i.e., $g\mu_B S$ for $g=2$ and $S=0.5$. This means that a small canting on adjacent Ru spins occurs and the saturation moments are not the full moments of the Ru^{5+} ions. The exact nature of the local structural distortions causing DM exchange coupling in Ru-2122 (see above) is not presently known.

At low applied fields, the $M(H)$ curve exhibits a typical ferromagneticlike hysteresis loop (Fig. 6) similar to that reported in Ref. 3. The positive virgin curve at low fields indicates clearly that SC is totally suppressed. Two other characteristic parameters of the hysteresis loops are shown in Fig. 6: namely, the remnant moment ($M_{\rm rem}=0.41\mu_B$/Ru) and the coercive field ($H_C=190$ Oe at 5 K). This $M_{\rm rem}$ is much larger than $M_{\rm rem}=0.035\mu_B$ obtained for $EuSr_2RuCu_2O_8$.[12] The same $M_{\rm rem}$ and H_C values (at 5 K) were obtained for the hop and quenched materials. Figure 4 shows the temperature dependence of $M_{\rm rem}$ (5 K), which disappears at $T_{\rm irr}$. The large $M_{\rm rem}$ ($0.41\mu_B$ at 5 K) in relation to the saturation moment ($M_{\rm sat}=0.89\mu_B$) is consistent with ferromagneticlike order in $EuCeRuSr_2Cu_2O_{10}$, although neutron diffraction measurements are required to precisely determine the nature of the magnetic order. $M(H)$ curves measured at various temperatures yield the $M_{\rm rem}(T)$ and $H_C(T)$ values which are plotted in Fig. 5. For both the asp and quenched samples $M_{\rm rem}(T)$ also disappears at $T_{\rm irr}$ and $H_C(T)$ becomes zero around 80 and 130 K, respectively (Fig. 5).

Above T_M(Ru), the $\chi(T)$ curve at 10 kOe for asp $EuCeNbSr_2Cu_2O_{10}$ has the typical paramagnetic shape and adheres closely to the Curie-Weiss (CW) law $\chi=\chi_0+C/(T-\theta)$, where χ_0 is the temperature independent part of χ, C is the Curie constant, and θ is the CW temperature. The net paramagnetic Ru contribution to $\chi(T)$ was obtained by subtracting $\chi(T)$ of $EuCeNbSr_2Cu_2O_{10}$ (the reference material) from the measured data. The procedure yields $\chi_0=0.0063$ and $C=0.57(1)$ emu/mol Oe and $\theta=146(1)$ K, which corresponds to an effective moment $P_{\rm eff}=2.13\mu_B$. Here θ obtained is in fair agreement with T_M, but $P_{\rm eff}$ is greater than the expected value of the low-spin state of Ru^{5+} and $S=0.5$ ($P_{\rm eff}=1.73\mu_B$).

C. Effect of Ce on the magnetic behavior of $Eu_{2-x}Ce_xRuSr_2Cu_2O_{10-\delta}$

As stated above, the compounds described here have been prepared simultaneously under the same conditions. Since

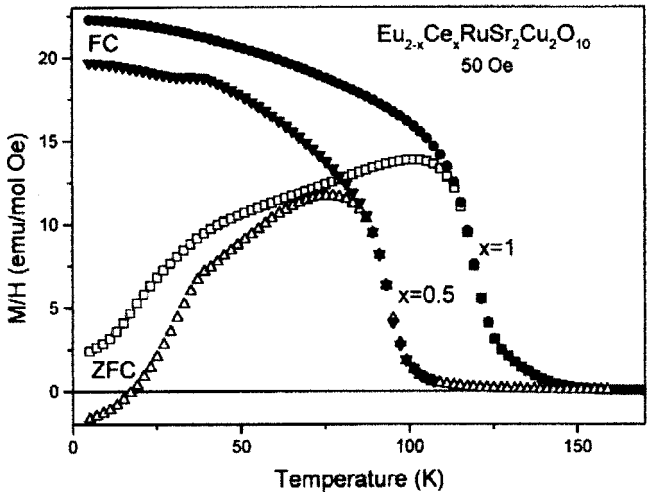

FIG. 7. ZFC and FC susceptibility curves for asp $x=1$ and $x=0.5$ samples, measured at 50 Oe.

the magnetic properties of the Ru-2122 system depend strongly on oxygen concentration,[5,6] the data presented here differ slightly from those reported in our previous publications. ZFC and FC magnetic as well as $M(H)$ measurements have been performed on all $Eu_{2-x}Ce_xRuSr_2Cu_2O_{10-\delta}$ ($x=0.4-0.9$) compounds. Generally speaking, the magnetic behavior of all materials is quite similar to these described in Figs. 3–6, and for the sake of brevity, we display the data obtained for $x=0.1$ and $x=0.5$ (Fig. 7). It is readily observed that for $x=1$, the magnetic properties due to the Ru are all *enhanced*, as compared to the $x=0.5$. The latter sample is SC and its ZFC branch starts from negative moments. The inflection in the FC branch agrees well with T_C determined from the ac curve (Fig. 1). The absence of a complete Meissner effect in the Ru-2122 system is discussed in length elsewhere.[16] However, this is of little interest in the present discussion.

The variation of $T_{\rm irr}$ and T_M as a function of Ce concentration in $Eu_{2-x}Ce_xRuSr_2Cu_2O_{10-\delta}$ is summarized in Fig. 8.

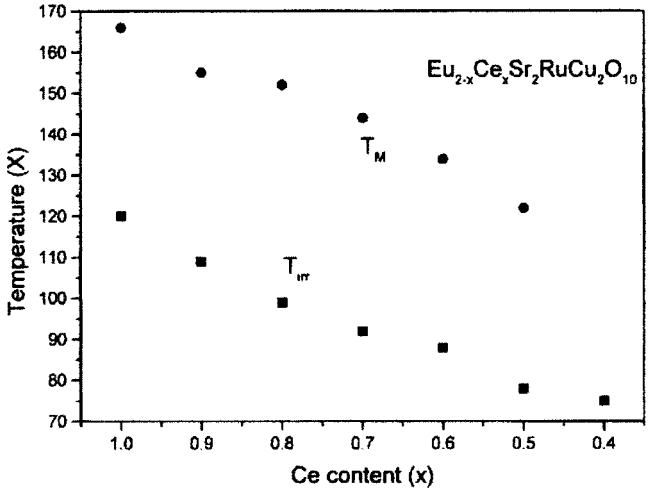

FIG. 8. T_M and $T_{\rm irr}$ as function of Ce in $Eu_{2-x}Ce_xRuSr_2Cu_2O_{10}$.

The enhancement of the magnetic properties is manifested by the monotonic rise of $T_{\rm irr}$ and T_M as x increases. $M_{\rm sat}$ values at 5 K, increase gradually with x, $M_{\rm sat}=0.43\mu_B$, $0.63\mu_B$, $0.60\mu_B$, $0.67\mu_B$, and $0.86\mu_B$ for $x=0.4$, 0.6, 0.7, 0.8, and 0.9, respectively. It is apparent that this trend is not affected by the SC state which is induced for $x=0.8$. For the $x=0.4$ sample, the ZFC and FC curves do not merge completely at T_M, but rather at 165 K, which indicates the presence of a tiny amount of $SrRuO_3$ (not detectable by XRD). Therefore, the T_M value for $x=0.4$ was not determined. In the paramagnetic range, the parameters extracted using the CW law have been obtained by subtracting the paramagnetic moment of the relevant Nb-2122 compound, as described above. It appears that the C and θ parameters for all materials are very close to those of $EuCeRuSr_2Cu_2O_{10}$, i.e., for $x=0.5$, $C=0.58$ emu/mol Oe ($P_{\rm eff}=2.15\mu_B$), and $\theta=134(1)$ K, indicating similar net paramagnetic Ru contribution in all Ru-2122 compounds. This is consistent with recent x-ray photoemission measurements which indicate clearly that the Ru^{5+} valence in $Eu_{2-x}Ce_xRuSr_2Cu_2O_{10-\delta}$ samples does not change with Ce concentration.[17]

D. Qualitative magnetic structure of $Eu_{2-x}Ce_xRuSr_2Cu_2O_{10-\delta}$

All magnetic parameters (such as T_M, $T_{\rm irr}$, or $M_{\rm sat}$) are shifted to higher values with increasing Ce. Our general picture is that all $Eu_{2-x}Ce_xRuSr_2Cu_2O_{10-\delta}$ compounds have a similar magnetic structure. Two scenarios may explain the trend presented in Fig. 8. (1) The small difference between Eu^{3+} and Ce^{4+} ionic radii discussed above decreases the mean Ru-Ru distance, and as a result, the magnetic exchange interactions can become stronger with increasing of x. (2) The magnetic properties of $Eu_{2-x}Ce_xRuSr_2Cu_2O_{10-\delta}$ are very sensitive to oxygen concentration[6] (see Fig. 3). The oxygen concentration for $x=1$ is fixed ($\delta=0$), whereas decreasing x to lower values may lead to an increase in oxygen deficiency (δ) and, as a result, to a decrease in T_M.

While our data described here do not include any determination of the magnetic structural order of the Ru sublattice in Ru-2122, the results are compatible with a simple model which is, however, of use in understanding the qualitative features at low applied fields. Starting from high to low temperatures, the magnetic behavior is basically divided into four regions. (i) At elevated temperatures, the paramagnetic net Ru moment is well described by the CW law, and the extracted $P_{\rm eff}=2.15\mu_B$ and $\theta=134-146$ K values practically do not alter with Ce. (ii) At T_M (depends on Ce content Fig. 8), which is deduced directly from the temperature dependence $M_{\rm sat}$ (Fig. 5), the Ru sublattice becomes AFM ordered. (iii) At $T_{\rm irr}$, which is Ce dependent (Fig. 8) and also varies with the external field, a weak ferromagnetism is induced, which originates from canting of the Ru moments. $T_{\rm irr}$ is defined as the merging point of the low-field ZFC and FC branches or, alternatively, at the temperature in which the remnant moment disappears. This canting arises from the DM antisymmetric superexchange interaction, which by symmetry follows from the fact that the RuO_6 octahedra tilt away from the crystallographic c axis.[3,11] At high magnetic field ($H>3000$ Oe) the irreversibility is washed out and the

$M(T)$ curves exhibit a ferromagneticlike behavior. (iv) At lower temperatures SC is induced. Figure 2 shows that $T_C < T_M$ depends strongly on Ce (as hole carriers) and on oxygen concentrations.[5,6] Below T_C, both SC and weak-ferromagnetic states coexist[3,10] and the two states are practically decoupled. This model is supported by our unpublished nonlinear ac susceptibility measurements, which show nonlinear signals up to T_M, and also from Mössbauer studies on ^{57}Fe-doped material.[18] However, the present interpretation differs completely from the phase separation of the AFM and FM nanodomain particle scenario, suggested in Ref. 16. Neutron diffraction measurements are required to precisely determine the properties of the magnetic order in the Ru-2122 system.

IV. SUMMARY AND CONCLUSIONS

The magnetic insulator parent $EuCeRuSr_2Cu_2O_{10}$ ($x=1$) is used to describe the coexistence of both SC and weak-ferromagnetism states in $Eu_{2-x}Ce_xRuSr_2Cu_2O_{10-\delta}$ ($x=0.4-1$). For $x=1$, $\delta=0$ and annealing under high oxygen pressure does not affect the magnetic properties, whereas T_M is enhanced by oxygen depletion. Hole doping of the Cu-O planes, which results in SC, can be optimized with appropriate variation of the Eu^{3+}/Ce^{4+} ratio and the optimally doped material is obtained for $Ce=0.6$. The magnetic structure of all materials studied is practically the same, but the magnetic parameters, such as T_M and M_{sat}, decrease with decreasing Ce content. Two steps in the magnetic behavior are presented. At T_M ranging from 125 K (for $x=0.5$) to 165 K (for $x=1$) all materials become AFM ordered. At T_{irr} (depends on Ce) a WFM state is induced, originating from canting of Ru moments. This canting can arise from the DM antisymmetric superexchange interaction and follows from the fact that the RuO_6 octahedra tilt away from the crystallographic *c* axis. A direct magnetic structure determination by neutron diffraction or ^{99}Ru Mössbauer spectroscopy studies is warranted to confirm our assumptions.

ACKNOWLEDGMENTS

This research was supported by the Israel Academy of Science and Technology and by the Klachky Foundation for Superconductivity.

[1] R. J. Cava, J. J. Krajewski, H. Takagi, H. W. Zandbergen, R. B. Van Dover, W. F. Peck, Jr., and B. Hessen, Physica C **191**, 237 (1992).
[2] L. Bauernfeind, W. Widder, and H. F. Braun, Physica C **254**, 151 (1995).
[3] I. Felner, U. Asaf, Y. Levi, and O. Millo, Phys. Rev. B **55**, R3374 (1997).
[4] E. B. Sonin and I. Felner, Phys. Rev. B **57**, R14 000 (1998).
[5] I. Felner, U. Asaf, F. Ritter, P. W. Klamut, and B. Dabrowski, Physica C **364-365**, 362 (2001).
[6] I. Felner, U. Asaf, Y. Levi, and O. Millo, Physica C **334**, 141 (2000).
[7] J. L. Pringle, J. L. Tallon, B. G. Walker, and H. J. Trodahl, Phys. Rev. B **59**, R11 679 (1999); C. Bernhard *et al.*, *ibid.* **59**, 14 099 (1999).
[8] X. H. Chen *et al.*, Phys. Rev. B **63**, 064506 (2001).
[9] A. Shengelaya *et al.* (unpublished).
[10] S. Y. Chen *et al.*, cond-mat/0105510 (unpublished).
[11] G. V. M. Williams and M. Ryan, Phys. Rev. B **64**, 094515 (2001).
[12] G. V. M. Williams *et al.*, (unpublished).
[13] C. S. Knee, B. D. Rainford, and M. T. Weller, J. Mater. Chem. **10**, 2445 (2000).
[14] I. Felner, U. Asaf, C. Godart, and E. Alleno, Physica B **259–261**, 703 (1999).
[15] Y. Hirai *et al.*, Phys. Rev. B (to be published).
[16] Y. Y. Xue, D. H. Cao, B. Lorenz, and C. W. Chu, Phys. Rev. B (to be published).
[17] G. V. M. Williams *et al.* (unpublished).
[18] I. Nowik, I. Felner, and U. Asaf, Hyperfine Interact. (to be published).